Spinar Paradigm and Gamma Ray Bursts Central Engine

V.M. Lipunov[1,2,3] and E.S. Gorbovskoy[1,2,3]
[1] *Sternberg Astronomical Institute, Moscow, Universitetsky pr. 13, Moskow 119992, Russia*
[2] *Moscow State University, Moscow, Universitetsky pr. 13, Moskow 119992, Russia.*
[3] *Moscow Union "Optic", Moscow, Valilov str 5/3, Moskow 119334, Russia.*

ABSTRACT

A spinar is a quasi-equilibrium collapsing object whose equilibrium is maintained by the balance of centrifugal and gravitational forces and whose evolution is determined by its magnetic field. The spinar quasi equilibrium model was recently discussed in the context of extralong X-ray plateu in GRB (Lipunov & Gorbovskoy, 2007).

We propose a simple non stationary three-parameter collapse model with the determining role of rotation and magnetic field in this paper. The input parameters of the theory are the mass, angular momentum, and magnetic field of the collapsar. The model includes approximate description of the following effects: centrifugal force, relativistic effects of the Kerr metrics, pressure of nuclear matter, dissipation of angular momentum due to magnetic field, decrease of the dipole magnetic moment due to compression and general-relativity effects (the black hole has no hare), neutrino cooling, time dilatation, and gravitational redshift.

The model describes the temporal behavior of the central engine and demonstrates the qualitative variety of the types of such behavior in nature.

We apply our approach to explain the observed features of gamma-ray bursts of all types. In particular, the model allows the phenomena of precursors, x-ray and optical flares, and the appearance of a plateau on time scales of several thousand seconds to be unified.

Key words:
black hole physics — Physical Data and Processes, gravitation — Physical Data and Processes, magnetic fields — Physical Data and Processes, relativity — Physical Data and Processes, gamma-rays: bursts — Sources as a function of wavelength, gamma-rays: theory — Sources as a function of wavelength

1 INTRODUCTION

.

The interest toward magneto-rotational collapse has increased appreciably in recent years in connection with the gamma-ray burst problem. It is now believed to be highly likely that long gamma-ray bursts may be associated with the collapse of a rapidly rotating core of a massive star and short gamma-ray burst are most likely to be results of the coalescence of neutron stars, which can be viewed as the collapse of a rapidly rotating object. We already pointed out in our earlier papers (Lipunova, 1997, Lipunova & Lipunov, 1998) the likely multivariate nature of, e.g., the coalescence of two neutron stars or neutron stars and black holes ("mergingology"), which may give rise to various forms of the temporal behavior of gamma-ray bursts. This is possibly corroborated by the recent complex classification of gamma-ray bursts (Gehrels et al., 2006).

Moreover, observations of the so-called precursors and x-ray flare certainly point to the complex nature of the operation if their central engines (Lazzati, 2005; Chincarini et al., 2007). ROTSE (Quimby et al., 1996a,) and MASTER (Lipunov et al., 2007) facilities observed optical flares in a number of cases.

All this triggers (mostly numerical) theoretical studies of collapse with the dominating role of rotation. Numerous attempts have been undertaken in order to incorporate effects due to rotation and magnetic fields in numerical computations, which are very difficult to understand intuitively and at the same time are extremely approximate because of the complex nature of the problem (Gehrels et al., 2006, Moiseenko et al., 2006; Duez et al., 2005, 2006).

Recently, (Lipunov & Gorbovskoy 2007) showed that spinar paradigm naturally explains not only the phenomenon of early precursors and flares, but even extraordinarily long x-ray plateaux.
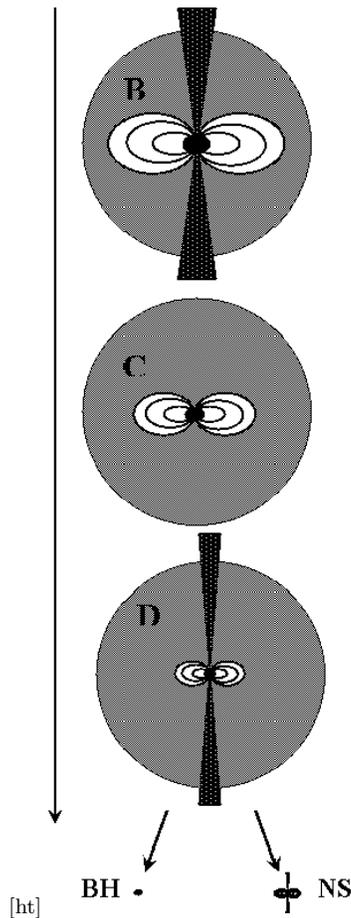
[ht]

Figure 1. Schematic view of the collapse of the rapidly rotating magnetized core of a massive star. Gray and black shaded areas show the envelope and core of the star, respectively. Before the collapse the size of the star is on the order of several solar radii and its iron core is one hundred times smaller (stage A). During the collapse centrifugal forces increase most rapidly, resulting in the formation of a spinar (stage B). Its formation is accompanied by anisotropic release of energy. Because of the dissipation of angular momentum the spinar decelerates and contracts (stage C). Its luminosity increases and a new jet forms whose energy release reaches its maximum near the gravitational radius. Depending on the core mass, the process results in the formation of a neutron star or an extremely rotating black hole.

In this paper we propose a pseudo-Newtonian theory of collapse based on a simple analytical model, which allows the maximum number of physical effects to be incorporated.

We use our model to interpret the data of observations of precursors (Lazzati, 2005), X-ray flares (Chincarini ey al., 2007), and some interesting gamma-ray bursts.

2   THE SPINAR MODEL.

The importance of incorporating magneto-rotational effects in collapse models was first pointed out in connection with the problem of quasar energy release and evolution (Hoyle and Fowler, 1963; Ozernoy, 1966; Morison, 1969; Ozernoy and Usov, 1973), and that of the ejection of supernova shells (Bisnovaty-Kogan; 1971, LeBlance & Wilson 1970).

In particular, it was pointed out that the collapse of a

star having substantial angular momentum may be accompanied by the formation of a quasi-static object – a spinar – whose equilibrium is maintained by centrifugal forces. Ostriker (1970) and Lipunov (1983) assumed the existence of low-mass spinars with close-to-solar masses. Lipunov (1987) made a detailed analysis the spin-up and spin-down of spinars in the process of accretion.

Lipunova (1997) developed a spinar model incorporating relativistic effects (which include the disappearance of magnetic field during the formation of a black hole), gave an extensive review of the research on the spinar theory, and tried to apply the spinar model to the gamma-ray event.

A spinar can be viewed as an intermediate state of a collapsing object whose lifetime is determined by the time scale of dissipation of the angular momentum. As Lipunova & Lipunov (1998) pointed out, the centrifugal barrier could explain the long (from several seconds to several hours) duration of the process of energy release in the central engines of gamma-ray bursts. It is remarkable that as it loses angular momentum a spinar (unlike, e.g., a radio pulsar) does not spin-down, but, on the contrary, spins up and this effect results in the increase of luminosity, which is followed by the luminosity decrease because of the disappearance of magnetic field, relativistic effect of time dilatation, and gravitational redshift near the event horizon.

Lipunova (1997) analyzes a model of a spinar in vacuum, which is justified for two neutron stars. However, in the case of a collapse of a core of a massive star the spinar is surrounded by the star's envelope and matter outflowing from its equator. We analyzed the interaction of a spinar with the ambient plasma in our earlier paper Lipunov (1987), from where we adopt the law to describe the dissipation of the spinar angular momentum .

Recently, Lipunov & Gorbovskoy (2007) developed a stationary spinar model, which allows for relativistic effects and maximum possible dissipation of the angular momentum of the spinar.

Below we abandon the quasi-stationary analysis and construct a non-stationary model of rotational collapse.

## 3   SPINAR SCENARIO OF MAGNETO-ROTATIONAL COLLAPSE. COLLAPSE OF A RAPIDLY ROTATING CORE.

Let us now qualitatively analyze the magneto-rotational collapse of a stellar core of mass M_{core} and effective Kerr parameter (Thorne et al., 1986)

$$a_0 \equiv \frac{I\omega_0 c}{GM_{core}^2} \tag{1}$$

(here $I = kM_{core}R_0^2$ is the moment of inertia of the core; ω is the angular velocity of rotation, and c and G are the speed of light and gravitational constant, respectively), and magnetic energy U_m.

In the case of conservation of the core angular momentum (which, of course, will be violated in our scenario), a remains constant.

Let α_m be the ratio of the magnetic energy of the core to its gravitational energy:

[ht]

Specific Angular Momentum (a)
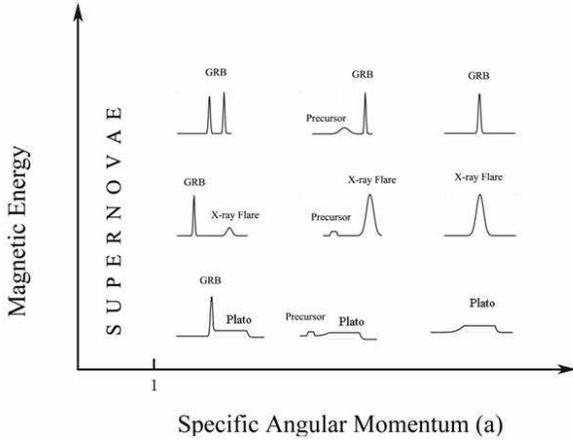
Figure 2. Qualitative variation of the characteristics of a gamma-ray burst and the accompanying phenomena shown on the magnetic field — effective Kerr parameter diagram.

$$\alpha_m \equiv \frac{U_m}{GM_{core}^2/R_A} \tag{2}$$

The total magnetic energy can be written in terms of the average magnetic field B penetrating the spinar:

$$U_m = \frac{B^2}{8\pi}\frac{4}{3}\pi R^3 = \left(\frac{1}{6}\right)B^2 R^3 \tag{3}$$

Note that in the approximation of magnetic flux conservation ($R^2 = const$), the magnetic-to-gravitational energy ratio remains constant during the collapse: $\alpha_m = const, U_m \propto R^{-1}$ without considering general-relativity effects.

Let the initial Kerr parameter $a_0 > 1$. In this case, direct formation of a black hole is impossible and the process of collapse breaks into several important stages (see Fig.1.):

A). Loss of stability by the core and free fall The time scale of this stage is on the order of the free-fall time

$$T_A = \sqrt{\frac{R_A^3}{GM_{core}}} \sim 100s \tag{4}$$

where R_A is the initial radius of the stellar core. Energy is virtually not radiated during the collapse, and gravitational energy transforms into kinetic, rotational, and magnetic energy of the core.

B). Halt of the collapse by centrifugal forces. Centrifugal forces stop free-fall collapse at the distance where

$$\omega^2 R_B = \frac{GM_{core}}{R_B^2} \tag{5}$$

It follows from this that the initial spinar radius is approximately equal to:

$$R_B = a^2 GM_{core}/c^2 = a^2 Rg/2 \tag{6}$$

In this process, half of the gravitational energy is released:

$$E_B = \frac{GM^2}{2R_B} - \frac{GM^2}{R_B} \approx \frac{GM^2}{2R_B} = \frac{1}{2a^2}M_{core}c^2 \tag{7}$$

if the energy is sufficient to "penetrate" the stellar envelope, i.e., if the momentum imparted to a part of the shell

exceeds the momentum corresponding to escape velocity. Let a part of the energy be converted into the energy of the jet ($\beta E_j = \beta E_B$)

$$\frac{\beta E_B}{v_j} > \theta_B^2 M_{shell}\sqrt{\frac{2GM}{R_{shell}}} \tag{8}$$

In this case a burst of hard radiation occurs.

We now substitute the burst energy (formula (7)) and spinar radius (6) into condition (8) to derive the "penetration" condition for the first jet:

$$1 < a_0 < \frac{1}{\theta_B^2}\frac{M_{core}}{M_{Shell}}\frac{C}{V_p} \tag{9}$$

where V_p is the escape velocity at the surface of the stellar envelope. In real situations $V_p = 2000 - 3000\ km/s$, $\frac{M_{core}}{M_{Shell}} \sim \frac{1}{10} - \frac{1}{3}$, and almost everything is determined by the jet opening angle. This simple estimate shows that the first penetration is highly likely even in the case of a large jet opening angle.

Because of the axial symmetry, the burst must be directed along the rotation axis and have an opening angle of θ_B^2. The duration of this stage is determined by the time it takes the jet to emerge onto the surface ($R_{shell} \sim 10 - 30s$) and the character of cooling governed by the structure of the primary jet and envelope.

The gamma factor of a jet emerging at the surface of the star can be approximately estimated using the energy conservation law (see a review by Granot, 2007):

$$E_{jet} \approx \Gamma^2\theta_B^2 M_{shell}c^2 \text{ and } \Gamma \sim E_{50}^{1/2}\theta_B^{-1}\left(\frac{M_{shell}}{M_\odot}\right)^{-1/2} \tag{10}$$

Here $E_{50} = E_B/10^{50}$ erg/s – jet energy.

The character of the spectrum is determined by the gamma factor of the jet.

If the initial Kerr parameter is large ($a \gg 1$) then energy $E_B \ll M_{core}c^2$ and the emerging jet is nonrelativistic allowing the event in question to be viewed as a precursor like it was done by Ramirez-Ruiz et al. (2002) and Wang & Meszaros (2007). Its spectrum can be estimated by the blackbody formula (eq. 16 in Wang & Meszaros, 2007):

$$T \sim 15L_{50}^{1/8}R_{11}^{-1/4}Kev$$

If the initial Kerr parameter is close to unity then the energy of the burst is high and the jet acquires a high gamma factor after penetration so that the flare should be interpreted as a gamma-ray burst. Although the jet that penetrates the star may be subrelativistic, however, a higher gamma-ray factor jet is to flood the already formed channel (the central engine continues to operate!). It is this evolved jet that should produce the gamma-ray burst provided that the spinar size is close to the gravitational radius.

We do not discuss the parameters of the jet, because this issue been addressed repeatedly by different authors (see reviews by Granot (2007) and Piran (2005)).

Only future numerical computations will make it possible to accurately determine the degree of anisotropy, i.e., e.g., the jet θ_B^2.

However, here we try to estimate the degree of anisotropy by determining the fraction of the spinar surface occupied by open field lines. Let us assume for a moment

that the spinar has a dipole moment equal to μ. Let us determine the Alfven radius R_{Alfven} of the jet from the condition of the balance of the jet ram pressure and magnetic-field pressure:

$$\frac{L_B}{(\theta_B^2 R^2 c)} \sim \frac{\mu^2}{8\pi R^6} \tag{11}$$

We use this formula to derive the Alfven radius:

$$R_{Alfven} \sim \theta_B^{1/2} (c\mu^2/2L_b)^{1/4}$$

We further assume that $\mu = BR^3/2$, where B is the intensity of magnetic field at the pole of the spinar, to obtain

$$R_{Alfven} \sim 3 \times 10^8 cm (\theta_B/0.01)^{1/2} B_{15}^{1/2} R_7^{1/2} R_7 L_{50}^{-1/4} \gg R_7$$

Here $B_{15} = B/10^{15} Gs, R_7 = R_B/10^7 cm$.

It is evident that all field lines passing inside this radius are closed. We use the approximation of the dipole field line equation to determine the size of polar regions enclosing open field lines:

$$\theta_{polar} \approx (R_B/R_{Alfven})^{1/2} \approx 0.03(\theta_B/0.01)^{1/4} B_{15}^{1/4} R_7^{1/4} L_{50}^{-1/8} \ll 1$$

Thus only 0.1% of the spinar surface participate in the formation of the jet, implying a very high degree of anisotropy of the process considered.

The newly formed spinar then evolves until its collapse without losing its axial symmetry.

C). Dissipative evolution of the spinar The spinar contracts as its angular momentum is carried away. Note that this process is accompanied by the increase of the velocity of rotation and luminosity of the spinar. At the same time, the magnetic dipole moment decreases and the luminosity stops increasing and begins decreasing. The energy release curve acquires the features of a burst.

The duration of this stage is determined by the moment of forces that carry away the angular momentum of the collapsar. In real situations turbulent viscosity and magnetic fields may play important part in the process.

The corresponding dissipation time scale (the spinar life time) is:

$$t_C = I_B \omega/K_{sd} \tag{12}$$

where K_{sd} is the characteristic torque of dissipative forces. It is clear that under the most general assumptions about the character of magnetic field the spin-down torque must be proportional to the magnetic energy of the spinar:

$$K_{sd} = \kappa_t U_m \tag{13}$$

where κ_t is the dimensionless factor that determines how twisted magnetic field lines are via which the angular momentum is dissipated.

Correspondingly, the total time scale of the dissipation of angular momentum (spinar lifetime (9)) is equal to:

$$t_C \sim \frac{I\omega}{U_m} \sim \frac{GM_{core}a_0^3}{c^3 \alpha_m \kappa_t} \tag{14}$$

D). Second burst Energy is released during dissipation, and the rate of this process increases progressively until general relativity effects — redshift and disappearance of magnetic field come into play.

As the luminosity increases, at a certain time instant the conditions of shell penetration (similar to condition (8)) become satisfied:

$$\frac{E_D}{c} > \theta_D^2 M_{shell} \sqrt{2\frac{GM}{R_{shell}}} \tag{15}$$

A second jet appears whose intensity reaches its maximum near the gravitational radius. Note that the effective Kerr parameter tends to its limiting value for the extremely rotating Kerr black hole: $a \to 1$.

The maximum luminosity can be written in terms of the dissipation of rotational energy near the gravitational radius:

$$L_D = \frac{M Rg^2 \omega}{\alpha M c^2} \sim \frac{\alpha_m c^5}{G} \tag{16}$$

It is better to write the condition of the penetration for the second jet in terms of pressure inequality:

$$\frac{L_D}{\theta_D^2 cR^2} > \frac{GM^2}{R^4} \tag{17}$$

Note that $\frac{c^5}{G} = 10^{59} erg/s$ is the so-called natural luminosity.

Of course, formula (15) does not include gravitational redshift, decay of magnetic field, etc.

The time scale near the maximum is:

$$T_D \sim \frac{M_{core} Rg^2 \omega}{U_m} = \frac{G M a^3}{c^3 \alpha_m} \tag{18}$$

Further fate of the star depends on its mass. If the mass exceeds the Oppenheimer–Volkoff limit the star collapses into a black hole. Otherwise (Lipunova & Lipunov, 1998) a neutron star forms, which cools after 10 seconds, continues to spin down in accordance with the following formula

$$K = \mu^2/R_l^3 \tag{19}$$

where μ is the magnetic dipole moment and $R_l = c/\omega$ is the radius of the light cylinder, and radiates as a common pulsar. In the case of constant magnetic field the luminosity of the pulsar should decrease in accordance with the following law:

$$L = \frac{\mu^2 \omega}{R_l^3} \sim t^{-2} \tag{20}$$

In the case of a coalescence of two neutron stars or a neutron star and a black hole the first stage (stage **A)** is very short, because the "fall" begins at a distance of several gravitational radii. Because of gravity-wave losses the components of the binary first approach each other to the radius of the last stable orbit and then merge to form a spinar. A small burst may occur at the time of stellar merging immediately before the spinar forms. This burst has the energy of:

$$\Delta E = \frac{G (M_1 + M_2)^2}{R_B} - \frac{GM_1^2}{R_1} - \frac{GM_2^2}{R_2} \sim 0.1(M_1 + M_2)c^2 \tag{21}$$

The qualitative picture of magneto-rotational collapse considered here can be illustrated by the following scheme (see Fig. 2.) in the coordinates U_m and a — the effective Kerr parameter.

The proposed scenario allows easy interpretation of the precursors and flares. In the case of large angular momentum $(a \gg 1)$ the initial radius is large and, correspondingly, the

energy release rate is low, allowing stage **B** to be interpreted as a precursor.

In the case of low angular momentum ($a >\sim 1$) the initial spinar radius is close to several gravitational radii and stage **B** must be interpreted as a gamma-ray burst, whereas the subsequent spinar burst **D** must be interpreted as a flare event.

It is remarkable that the time interval between the two bursts is always determined by the duration of dissipation of angular momentum (14), and, consequently, a rest-time measurement immediately yields a relation between the Kerr parameter and the fraction of magnetic energy:

$$\frac{\alpha_m}{a_0^5} = \frac{\Delta t c^5}{G M_{core} \kappa_t} \cong 10^{-6} \frac{M}{10 M_\odot} \Delta t_2^{-1} \kappa_t \quad (22)$$

where $\Delta t_2 = \Delta t / 100s$.

Correspondingly, the characteristic magnetic field at the collapse time (near Rg) is equal to:

$$B = \left(\frac{Rg}{R_{core}}\right)^{-2} \sqrt{\frac{\alpha_m G M^2}{6 R_{core}^4}} \approx 2 \cdot 10^{15} Gs \cdot \alpha_{-6}^{1/2} \left(\frac{M_{core}}{M_\odot}\right)^{-3/2} \quad (23)$$

where $\alpha_{-6} = \alpha_m / 10^{-6}$.

The proposed scenario allows the observed variety of gamma-ray bursts, precursors, and flares to be reduced to just two parameters: magnetic field and initial angular momentum.

Let us considered firstly two upper line of the diagram (Fig.2). In the case of weak magnetic field and large angular momentum (the right side of the middle line) the first burst is weak (because of the high centrifugal barrier) and the resulting jet does not penetrate the stellar envelope – there are no precursors to be observed. This is followed by slow collapse (magnetic field is weak), which results in a weak x-ray rich burst. As the initial angular momentum decreases (we move leftward in the diagram along middle line) the energy released at the centrifugal barrier increases and the jet becomes capable of "penetrating" the stellar envelope. The first burst should act as a precursor. The precursor should be separated from the gamma-ray burst, because the time scale of the dissipation of angular momentum is long in the case of a weak field. As angular momentum decreases (we move further leftward along the horizontal middle line) the precursor energy increases and at $a >\sim 1$ the precursor energy exceeds $10^{51-52} erg$ and it shows up as a gamma-ray burst with the subsequent collapse of the spinar leading to X-Ray flare or an X-ray plateau event (the bottom-line Lipunov & Gorbovskoy, 2007) with more weak field.

In the case of even stronger magnetic field, the flare approaches a gamma-ray burst, its energy grows and the flare itself becomes a part of the gamma-ray burst (the top-left corner). If we move rightward, angular momentum grows and the first flare loses energy and becomes a precursor close to the second flare, which, in turn, actually becomes a gamma-ray burst.

In the case of very large angular momentum (the top-right corner) the energy of the precursor is insufficient for penetrating the envelope and we have a burst without satellites. The duration of energy release increases with decreasing strength of magnetic field and the burst becomes softer (we come to the bottom-right corner) and turn into isolated long X-ray plateau.
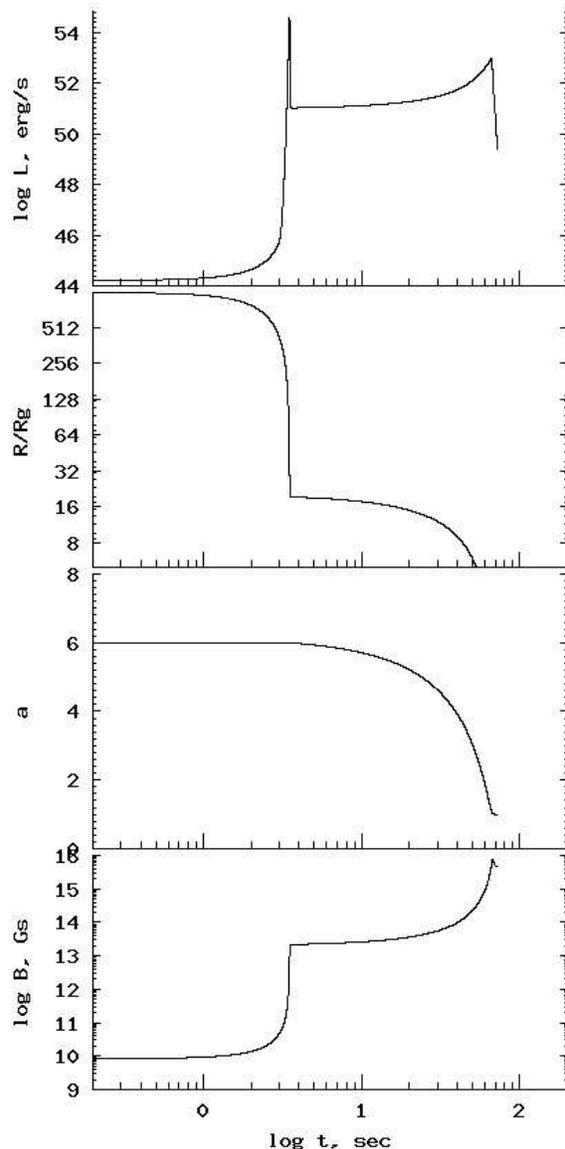
[ht]

Figure 3. Computation of the collapse of a 7 solar mass core with effective Kerr parameter a_0=6 and magnetic-to-gravitational energy ratio α_m=10^{-4}. From top to down: energy release as viewed by an infinitely distant observer, radius, effective Kerr parameter, and the average magnetic field strength.

4 ONE POINT PSEUDO-NEWTONIAN NONSTATIONARY SPINAR MODEL OF THE MAGNETO-ROTATIONAL COLLAPSE.

The aim of our model is to provide a correct qualitative and approximate description of magneto-rotational collapse, which would allow us to follow the evolution of the rate of energy release of the collapsing object and demonstrate the diverse nature of the central engine. Note that the spinar is born and dies in a natural way as a result of the solution of nonstationary problem.

Let us assume that at the initial time instant we have a rotating object (it may be a core of a massive star that has become unstable, or a merged neutron star, or the massive disk around a black hole). The object has the mass of , radius R_{core}, angular momentum $I\omega$, dipole momentum μ_0, and Kerr parameter a_0.

a). Dynamic Equation

We write the equation of motion in the post-Newtonian approximation:

$$\frac{d^2 R}{dt^2} = F_{gr} + F_c + F_{nuclear} + F_{diss} \tag{24}$$

where F_{gr} is the gravitational acceleration, F_c, the centrifugal acceleration, and $F_{nuclear}$, the pressure of matter.

Several attempts have been made to propose a pseudo-Newtonian potential to simulate the Kerr metrics (see Artemova et al., 1996). In our model we use effective acceleration in the form proposed by Mukhopadhyay (2002) for particles moving in the equatorial rotation plane:

$$F_{gr} = -\frac{GM}{x^3} \frac{(x^2 - 2ax + a^2)^2}{(\sqrt{x}(x-2) + a)^2} \tag{25}$$

where $x = 2R/R_g$. This formula corresponds to the potential of Paczynski & Wiita (1980) for a nonrotating black hole.

Next terms:

$$F_c = \omega^2 R \tag{26}$$

$$F_{nuclear} = \frac{1}{\rho}\frac{dP}{dr} \approx \frac{P}{\rho R} \tag{27}$$

Pressure of gas, which includes thermal pressure, can be written as kinetic energy of particles computed using relativistic invariant (Zel'dovich, Blinnikov, Shakura 1980):

$$P \approx \rho(\sqrt{c^4 + b\rho^{2/3} + (Q/M)^2} - c^2) \tag{28}$$

The second and third terms under the radical sign allow for the pressure of degenerate gas and thermal energy, respectively.

Let us now rename constant b:

$$b = \left(\frac{4\pi}{3}\right)^{2/3} G^2 M_{Class}^{4/3} \tag{29}$$

We actually use the formula for the pressure of partially degenerate Fermi gas with the contribution of thermal pressure. It is clear that the equation of real nuclear matter cannot be described by such a simple formula. However, we managed, by fitting appropriate values of constant b,to obtain neutron stars with quite plausible parameters (see Appendix 1). By varying constant b we can, in particular, vary the Oppenheimer—Volkoff limit for cool nonrotating neutron stars. We put $M_{OV} = 2M_\odot$ in this paper for cool nonrotating neutron stars.

Of course, one must bear in mind that the real Oppeheimer—Volkoff limit depends both on the velocity of rotation of the neutron star and on its thermal energy (Friedmann et al., 1985). In our model this dependence is qualitatively consistent with the numerical results obtained earlier.

We finally introduce dissipative force F_{diss}:

$$F_{diss} = -\frac{1}{\tau}\left(\frac{dR}{dt}\right) \tag{30}$$

It is clear from physical viewpoint that after reaching the centrifugal barrier the core undergoes extremely strong oscillations with a time scale of $1/\omega$. This process is accompanied by the redistribution of angular momentum and complex nonaxisymmetric motions, which must ultimately result in the release of half of the gravitational energy and formation of a quasi-static cylindrically symmetric object — a spinar. A detailed analysis of this transition is beyond the scope of our simple model. We just introduce a damping force assuming that its work transforms entirely into heat so that our model correctly describes the total energy release during the formation of the spinar, but is absolutely unable to describe the temporal behavior at that time. We actually assume that:

$$\tau = 2\pi\chi/\omega \tag{31}$$

Throughout this paper, $\chi = 0.04$ unless otherwise indicated.

b) Angular momentum loss equation

The decrease of the angular momentum of the spinar (collapsar) is due to the effect of magnetic and viscous forces. In this paper we assume that dissipation of angular momentum is due to the effective magnetic field. In this case, the breaking torque in a disk-like object is equal to (see Lipunov, 1992)

$$K = \int\limits_{R_{\min}}^{\infty} \frac{B_z B_\phi \, dS}{4\pi} = \frac{1}{2}\int\limits_{R_{\min}}^{\infty} B_z B_\phi R \, dR, \tag{32}$$

where B_z and B_ϕ — z and ϕ are the components of magnetic field.

We now introduce the magnetic moment μ of the spinar. Hereafter, for the sake of simplicity, we write our equations as if the spinar had a dipole magnetic field. However, our equations remain unchanged if we simply use some average magnetic field of the spinar and characterize this field by the spinar magnetic energy U_m mentioned above. This is true for the breaking torque that we use below.

Let $B_z B_\phi = \kappa_t B_d$, where $B_d = \frac{\mu}{R^3}$ is dipolar strength of the magnetic fields. The breaking torque is then equal to (see Lipunov, 1987, 1992 see below)

$$K = \kappa_t \frac{\mu^2}{R_t^3}, \tag{33}$$

where $\kappa_t \sim 1$ and R_t is the characteristic radius of interaction between the magnetic field and ambient plasma:

$$
\begin{aligned}
&R_t = R_{Alfven} \text{ is the Alfven radius (Propeller)}\\
&R_t = Rc = \left(\frac{GM}{\omega^2}\right)^{1/3} \text{ is the corotation radius (Accretor)}\\
&R_t = R_l = \frac{c}{\omega} \text{ is the radius of the light cylinder (Ejector)}
\end{aligned} \tag{34}
$$

In the case of a spinar the Alfven radius is smaller than or on the order of the stellar radius and is of little importance in the situation considered.

In the case of a collapsing core the effective interaction radius must be close to the corotation radius, which, in turn, is close to the spinar radius in accordance with tits

equilibrium condition. Therefore the retarding torque can be written as:

$$K = \frac{\kappa_t \mu^2 \omega^2}{GM} = \frac{\kappa_t \mu^2}{R_B^3} \tag{35}$$

And the corresponding dissipation time scale is:

$$T_C = \frac{I_B \omega^2}{\mu^2 / R_B^3} \tag{36}$$

Hence the equation of variation of the spinar angular momentum becomes (Lipunov, 1987):

$$\frac{dI\omega}{dt} = -\frac{\mu^2}{R_c^3} = -\frac{\kappa_t \mu^2 \omega^2}{GM} \tag{37}$$

Some authors (Woosly, 1993; Narayan et al., 2001) consider a situation where accretion continues onto the newborn black hole at a rate of up to 10^{-1}M/yr. In just the same way accretion may continue onto the spinar. The equation of the variation of the angular momentum of the an accreting spinar was first derived by (Lipunov, 1987 equation 123):

$$\frac{dI\omega}{dt} = -\frac{\mu^2}{R_c^3} = -\frac{\kappa_t \mu^2 \omega^2}{GM} + \overset{\bullet}{M} \sqrt{GMR}$$

where $\overset{\bullet}{M}$ is the disk-accretion rate. It was shown in the same paper that accretion dose not change dramatically spinar evolution and hereafter we neglect accretion. The effect of accretion should always be important if the accretion time is much shorter than the time scale of dissipation of angular momentum, $t_{acctretion} \sim \frac{M_{core}}{\overset{\bullet}{M}} < T_C$ However, in this case the very process of accretion is the process of the formation of the spinar. Note that our scenario differs substantially from that of Woosley (1993), who considers accretion to be of importance, because it is the process that determines the energetics of the gamma-ray burst. A spinar is a collapsing (but not a collapsed!) stellar core.

In other words, a spinar is by itself an "accretion disk". Of course we may complicate the model in the future, but we prefer to stop our coarse (but physically transparent) approximation here and ignore accretion.

The retarding torque written in this form gives the absolute upper limit for the possible spin-down of the spinar.

If the mass of the spinar is below the Oppenheimer—Volkoff limit, a neutron star forms ultimately, which spins down in accordance with the following magnetodipole formula:

$$\frac{dI\omega}{dt} = -\frac{\kappa_t \mu^2}{R_l^3} \tag{38}$$

c). Magnetic Field Evolution

As is well known (Ginsburg and Ozernoy, 1963) magnetic field must disappear in the process of collapse.

In the Newtonian approximation in the case of magnetic-flux conservation, the dipole moment behaves as:

$$\mu \sim BR^3 \sim BR^2 R \sim R \tag{39}$$

With relativistic effects taken into account, magnetic field vanishes not at zero, but when the star reaches the event horizon. Manko and Sibgatullin (1992) computed the evolution of the dipole magnetic field of a rotating body (in the Kerr metrics).

We can use the following simple formulas as the first approximation:

$$\mu = \mu_0 \frac{R - R_{\min}/2}{R_0 - R_{\min}/2} \tag{40}$$

Here $R_{\min}$ is the equatorial radius of the event horizon. Given that $R_0 \gg R_{min}$, this formula correctly describes the behavior of the dipole moment and yields zero magnetic field at the event horizon.

However, this law implies too fast decrease of magnetic field and we use the following modified law of magnetic-field decay adopted from Ginsburg and Ozernoy (1963):

$$\mu \sim \mu_0 \left(\frac{R_0}{R}\right)^2 \frac{\xi(x_0)}{\xi(x)} \tag{41}$$

where $\xi(x) = \frac{x_{\min}}{x} + \frac{x_{\min}^2}{2x^2} + \ln\left(1 - \frac{x_{\min}}{x}\right)$ and $x_{\min}$ is the radius of horizon for current Kerr parameter.

In this paper we neglect the effects of generation of magnetic fields.

d).Energy losses

.

The release of energy in the process of collapse is initially due to the dissipation of kinetic energy of the impact onto the centrifugal barrier and to spinar spin-down due to magnetic forces:

$$L_0 = \frac{1}{\tau} M \left(\frac{dR}{dt}\right)^2 \quad \text{before the formation of the spinar} \tag{42}$$

$$L_0 = \frac{\mu^2}{R_{\min}^3} \omega \quad \text{after the formation of the spinar} \tag{43}$$

Where invariably $R_{\min} = R_c$ if the core mass exceeds the Oppenheimer—Volkoff limit.

A distant observer would record lower luminosity because of gravitational redshift and time dilatation.

We adopt the following observed luminosity:

$$L_\infty = \alpha^2 L_0 \tag{44}$$

where α is the time dilatation function — the ratio of the clock rate of reference observers to the world time rate at the equator of the Kerr metrics (Thorne et al., 1986):

$$\alpha = \sqrt{\frac{x^2 + a^2 - 2x}{x^2 + a^2}} \tag{45}$$

If the core mass is below the Oppenheimer—Volkoff limit, the spinar ultimately evolves into a neutron star and its luminosity is given by the following magnetodipole formula:

$$L_0 = \kappa_t \frac{\mu^2}{R_l^3} \omega \tag{46}$$

We finally consider the case where rotation is so slow that the spinar does not form at all.

In this case direct collapse occurs. We pointed out above that Lipunova (1997) was the first to address the problem of electromagnetic burst with the allowance for general relativity effects. In the case of direct collapse rotational motion is of no importance, because the star makes less than a single rotation before it is under the event horizon.
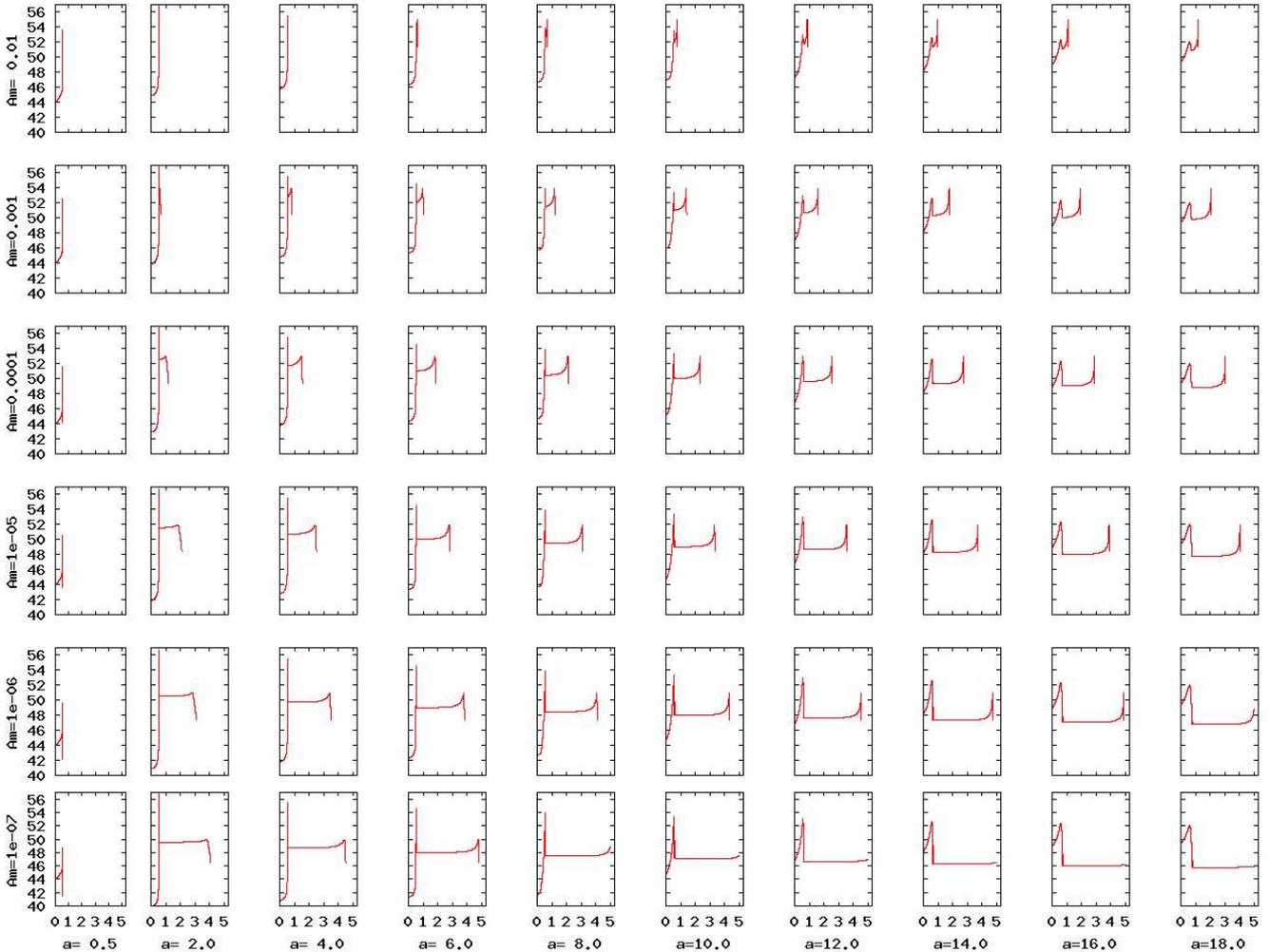
Figure 4. Operation of the central engine. Results of the computation of energy release (luminosity-time in logarithmic coordinates) during the collapse of 7 $M_\odot$ stars.

However, this case is characterized by large radial variation of the dipole moment:

$$L = \frac{2}{3c^2}\left(\frac{d\mu}{dt}\right)^2 \tag{47}$$

To convert this value into the observed luminosity we must take into account gravitational redshift and the Dopple effect due to the emitter falling in a virtually Schwartzshieldian metrics (Lipunova, 1997).

5   COLLAPSE OF A MASSIVE CORE ($M > M_{OV}$).

Let us first consider the case where the core mass exceeds substantially the Oppenheimer—Volkoff limit. We adopt the initial core mass of $1000Rg$ as the initial conditions for our set of differential equations. Figure 3 shows the computed variation of the radius, Kerr parameter, and average magnetic field for several arbitrary initial core parameters as functions of proper time (without the allowance for the time dilatation factor). Diagram 4 shows the computed evolution

of the central engine for a wide range of models. Let us emphasize several important points. First, the collapse of such cores ends by the formation of an extremely rotating Kerr black hole. Of course, this event shifts to infinitely distant time in the rest frame.

The diagram (Fig.4) fully corroborates our qualitative scenario (Fig. 2) and demonstrates a large variety of the time scales and energies of precursors, gamma-ray bursts, and flares. The results of computations of the energy release in direct collapse ($a_0 < 1$) confirms the short duration and low power of the flare. Note that the total energy does not exceed $10^{-4}Mc^2$ for almost all values of magnetic field. Evidently, in this case the appearance of jets and of the gamma-ray burst phenomenon is difficult to imagine. Such a collapse would rather result in a common supernova event.

However, the events acquire an increasingly dramatic turn with increasing moment. At $a_0 > 1$ centrifugal forces sooner or later exceed the gravitational forces, halt the collapse to give time and opportunity for enormous energy of about $\sim 0.1Mc^2$ to be radiated during the halt of the collapse. In this case a spinar is born and the relativistic jet penetrates the envelope of the star and triggers a gamma-

ray burst. The magnitude of the first burst depends on the initial spinar radius exclusively, which to a first approximation is determined only by the moment, as is evident from the diagram. All systems in the same column have the same burst energy. Magnetic field then takes the reigns of government and determines the rate of dissipation of angular momentum and becomes the main factor to determine further evolution of the core. As magnetic moment decays, the core radius decreases and magnetic luminosity increases until it reaches its maximum (at $R \sim Rg$) whose magnitude is determined by the magnetic field exclusively. This is also evident from the diagram. After that the luminosity decreases abruptly because of relativistic effects near the event horizon (decay of the field, gravitational redshift, and time dilatation). It is the ratio of the energies of the first and second flare that determines the entire zoo (all the variety) of flare, precursor, and burst events. In the extreme case of a strong magnetic field (Eq.23) and comparatively small momentum ($1 < a_0 < 6$) both flares are very short, narrow, and separated by a short time interval of $\sim$1-10s. It is thus impossible in this case to separate the burst from the precursor or flare and we must view the event as a double gamma-ray burst.

If we move rightward on the diagram in the direction of increasing momentum the initial spinar radius increases (for systems with $\sim 100Rg$ large precursors), the gravitational energy released decreases, and the first flare becomes weaker. We thus fall into the domain of precursors: ($\alpha_m \sim 10^{-2} - 10^{-4}, 10 < a_0 < 20$). The greater is the angular momentum and the stronger the magnetic field, the greater is the separation between the precursor and the gamma-ray burst. Luminosity remains virtually constant between the precursor and the gamma-ray burst.

If, on the other hand, we move downward from the domain of double gamma-ray bursts, thereby decreasing the magnetic-field strength, increasing the time interval between the primary and secondary bursts, and decreasing the intensity of the second burst, we come into the extended domain of gamma-ray bursts ($\alpha_m \sim 10^{-4} - 10^{-7}, 2 < a_0 < 14$). If its initial angular momentum is comparatively small, the spinar has an initial radius of $\sim 10Rg$ and the first burst must be very powerful. Magnetic field, however, is weak and the power of the second burst would suffice only to produce X-ray flares. In the case of too weak fields ($\alpha_m \leqslant 10^{-7}$) the second burst is virtually absent, allowing some bursts (e.g., GRB070110 and GRB050904, see below for details) to exhibit a long ($\sim 10^4$) x-ray plateau.

Finally, the bottom-right corner is occupied by the systems where the energy of neither the first nor the second flare is too low for a gamma-ray burst. These cores ($\alpha_m \leqslant 10^{-6}$, $a_0 > 14$) may produce either an x-ray burst with a precursor or unusual supernovas.

6   COLLAPSE OF A RAPIDLY ROTATING INTERMEDIATE-MASS CORE ($M > \sim M_{OV}$) (SUPERNOVA CASE).

As it was marked (Lipunova, 1997; Lipunova & Lipunov, 1998; Vietri & Stella, (1998) - a "supranova" scenario), as Oppenheimer—Volkoff limit for fast rotating neutron star is higher, then massive NS temporal formation is possible.
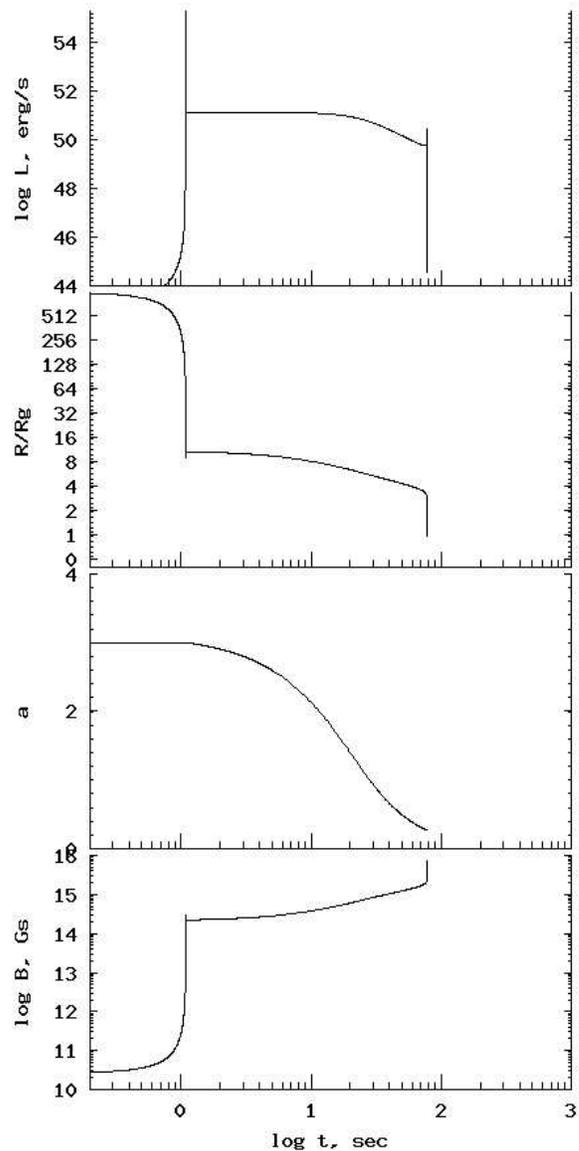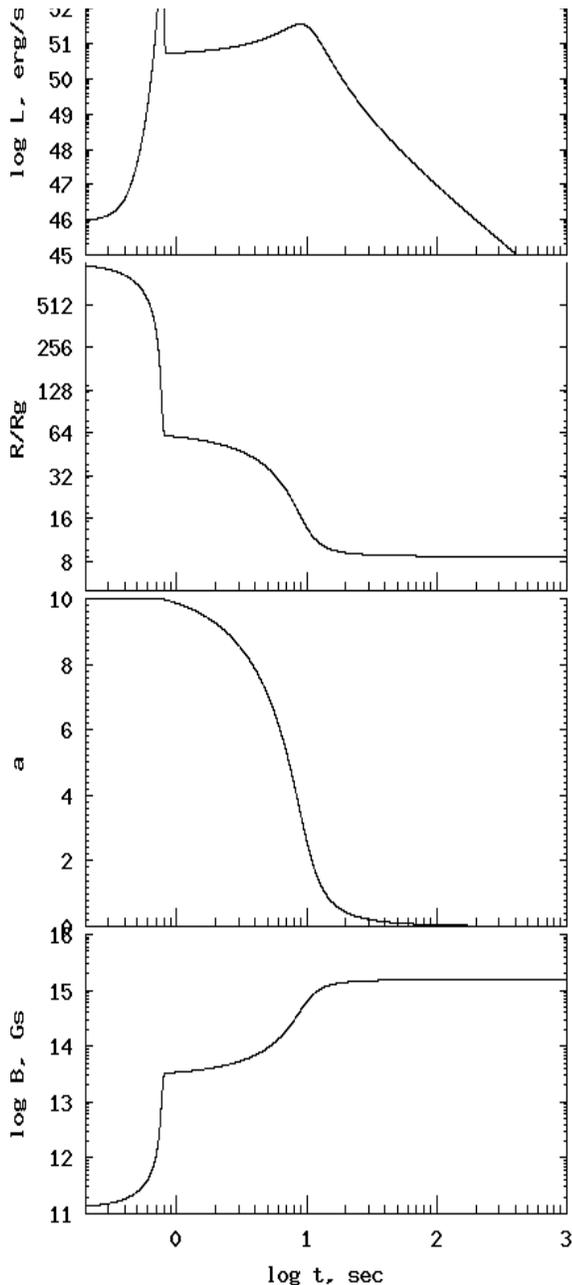

[!h]

Figure 5. Computation of the collapse of a $2.2M_\odot$ star. The initial effective Kerr parameter and initial magnetic-to-gravitational energy ratio are equal to $a_0 = 3$ and $\alpha_m = 10^{-4}$ respectively.

Having lost its rotational moment, the star collapse in to the black hole.

For example let us consider a fast rotating core collapse with mass $2.2M_\odot$. We should remind that, for distinctness, we use the state equation with Oppenheimer—Volkoff limit equal to 2.0 Solar masses (for non-rotational neutron star).

Practically, that means that, spinar equilibrium at last stages of evolution is maintained both centrifugal and nuclear forces and may be by thermal pressure.

Fig.5 demonstrates the result of that core collapse calculation. The heavy neutron star exists for about 100 seconds. As magnetic momentum looses lead to rotation acceleration, its magneto-rotating luminosity after initial plateau

[ht]

Figure 6. Computation of the collapse of a $1.5M_\odot$ star. The initial effective Kerr parameter and initial magnetic-to-gravitational energy ratio are equal to $a_0 = 10$ and $\alpha_m = 10^{-3}$, respectively.

begins to decrease (the nuclear pressure doesn't allow neutron stars-spinar to compress strongly).

But after near 100 seconds effective Kerr parameter becomes less than unity and relativistic effects result in rapid direct collapse of neutron star into the black hole.

7   COLLAPSE OF A RAPIDLY ROTATING LOW-MASS CORE $(M < M_{OV})$.

The collapse of a low-mass star is ultimately halted by the pressure of degenerate matter. However, even in this case fast rotation plays important part. In a number of cases,

a neutron star does not form directly, but first a spinar, which then transforms into a neutron star losing angular momentum. Such a collapse does not end by abrupt decrease of luminosity (as in the cases considered above), but has a long tail: $L \sim t^{-2}$.

In this example we consider the collapse of a $1.5M_\odot$ core into a neutron star (Fig.6). The process results in the formation of a neutron star of radius $\sim 8.5Rg(38km)$. Thus the problem acquires yet another characteristic radius — R_{NS} (the nonrotating neutron star radius).

If centrifugal forces less then nuclear pressure ($R_{NS} > R_{Spinar}$), and this is quite possible with strong fields and small angular momenta, the neutron star forms directly and the light curve has only one maximum followed by a t^{-2} decrease due to uniform dissipation of the angular velocity of the NS. Such systems are located in the bottom-left corner of diagram (Fig.7). $(\alpha_m \geqslant 10^{-3}, a_0 < 6)$.

If $R_{NS} < R_{Spinar}$, the process again acquires a two-burst pattern. However, it does not resemble the collapse of a massive core. This is due to the fact that if the radius of the NS is $\sim 10Rg$ no second burst is to be expected near Rg. Hence we have no systems with precursors and gamma-ray bursts occur only in systems with small initial momenta $(a < 12)$.

Some systems with intermediate rotation and strong field $(\alpha_m \geqslant 10^{-4}, 6 < a_0 < 12)$ may produce a weak x-ray flare. This flare is not observed in systems with small angular momentum, because in these cases the height of the plateau exceeds that of the flare.

In other cases the energy of any flare is hardly sufficient for it to penetrate the envelope, and supernovas are observed.

8   STATISTICAL PROPERTIES OF PRECURSORS, FLARES, AND GAMMA-RAY BURSTS.

An analysis of BATSE data (Lazzati, D., 2005) shows that up to 20 percent of long gamma-ray bursts have precursors preceding the trigger time by up to $200s$. Chincarini et al., (2007) found about 30 flux increase events (optical flares) from Swift observatory data.

There are no more doubts that at least a substantial part of these phenomena are associated with the peculiarities of the operation of the "central engine".

8.1   Precursors.

Numerous observations of gamma-ray bursts show a complex structure in their temporal behavior, which is impossible to explain in terms of a single burst, formation of a jet, and development of a system of shocks in this jet. For example, the model associated with the emergence of the tip of the bow shock onto the star's surface (Ramirez-Ruiz et al., 2002; Waxman & Meszaros (2003)) can explain precursors that are close to the time of the gamma-ray burst (GRB-time), but not the early precursors preceding the main GRB by $100 - 200s$ (Xiang-Yu Wang & Meszaros, 2007). The latter authors proposed a model where early precursors appear as a result of the fallback of a part of the star's shell.
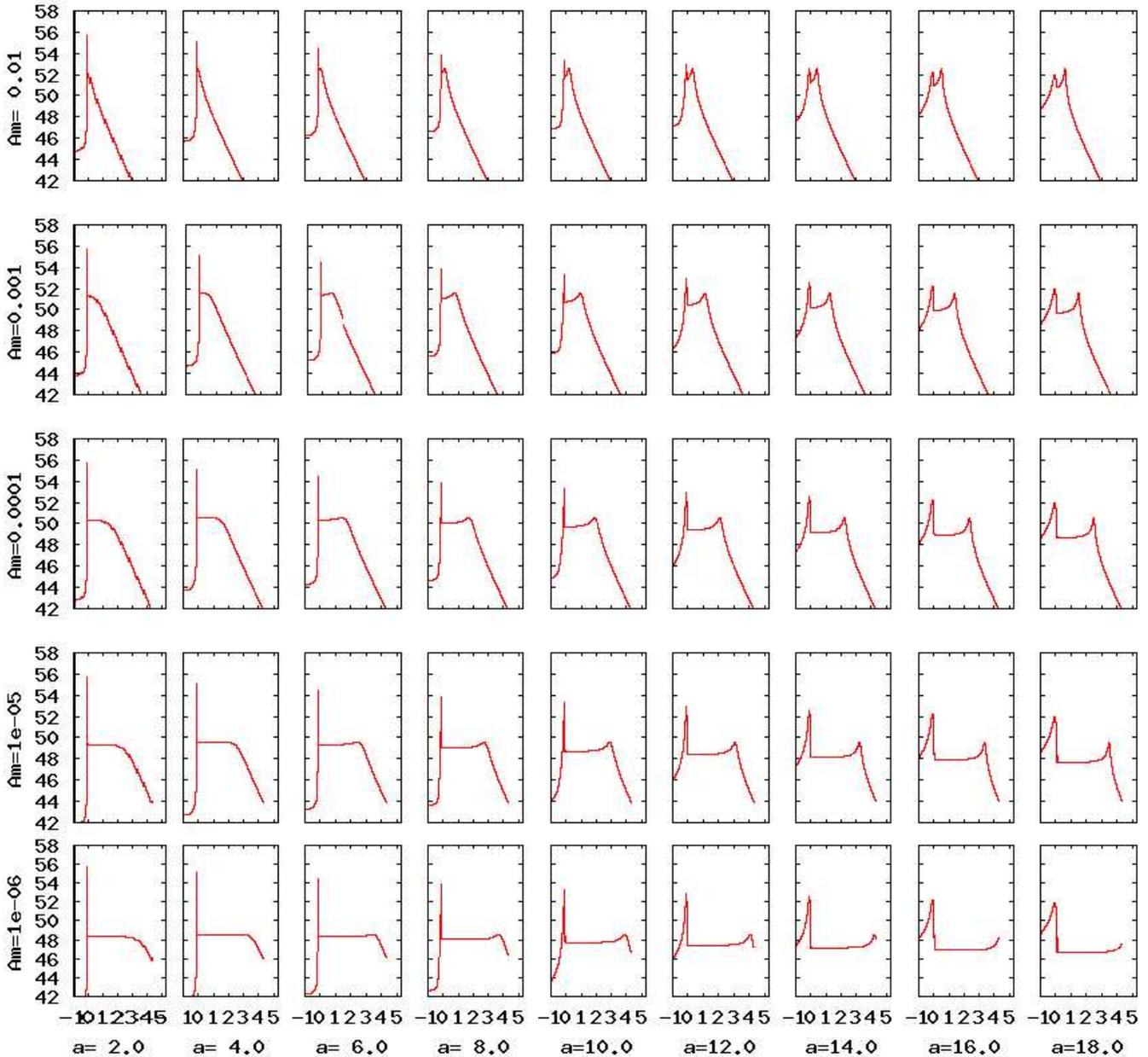
Figure 7. Operation of the central engine. Results of the computation of energy release (luminosity-time in logarithmic coordinates) in the process of the collapse of a core into a $1.5 M_\odot$ neutron star with different values of the effective Kerr parameter (a) and initial magnetic-to-gravitational energy ratio (α_m). We set the initial core radius equal to $1000 Rg$. The first and second flares correspond to the formation of the spinar and neutron star, respectively. At the end of the process, energy release always begins to obey the magnetodipole law corresponding to the spin-down of the neutron star, i.e., the pulsar. Computation of the collapse of a $1.5 M_\odot$ star. The initial effective Kerr parameter and initial magnetic-to-gravitational energy ratio are equal to $a_0 = 10$ and $\alpha_m = 10^{-3}$, respectively.

Our proposed scenario naturally explains the phenomenon of precursors and flares. In the case of large angular momentum ($a \gg 1$) the initial radius is large and, correspondingly, the energy release is low, allowing stage **B** to be interpreted as a precursor phenomenon.

In this case, the following condition must evidently be satisfied:

$$T_{pre} = T_B = T_{GRB} \left(\frac{R_B}{Rg} \right)^{3/2} = T_{GRB} \frac{E_{GRB}}{E_B} = T_{GRB} \frac{T_{90GRB}}{T_{90Pre}} \frac{\theta^2_{GRB}}{\theta^2_{Pre}} \quad (48)$$

where T_{pre}, T_{GRB}, F_{90}, and θ are the observed fluence, and

the jet opening angle of the gamma-ray burst or precursor, respectively. Note that the slope of the latter relation does not depend on the redshift of the gamma-ray burst.

In the model considered a precursor is defined as the initial energy release when centrifugal forces halt the collapse of the core (stage B) in the case where

$$GM^2/R \ll Mc^2 \quad (49)$$

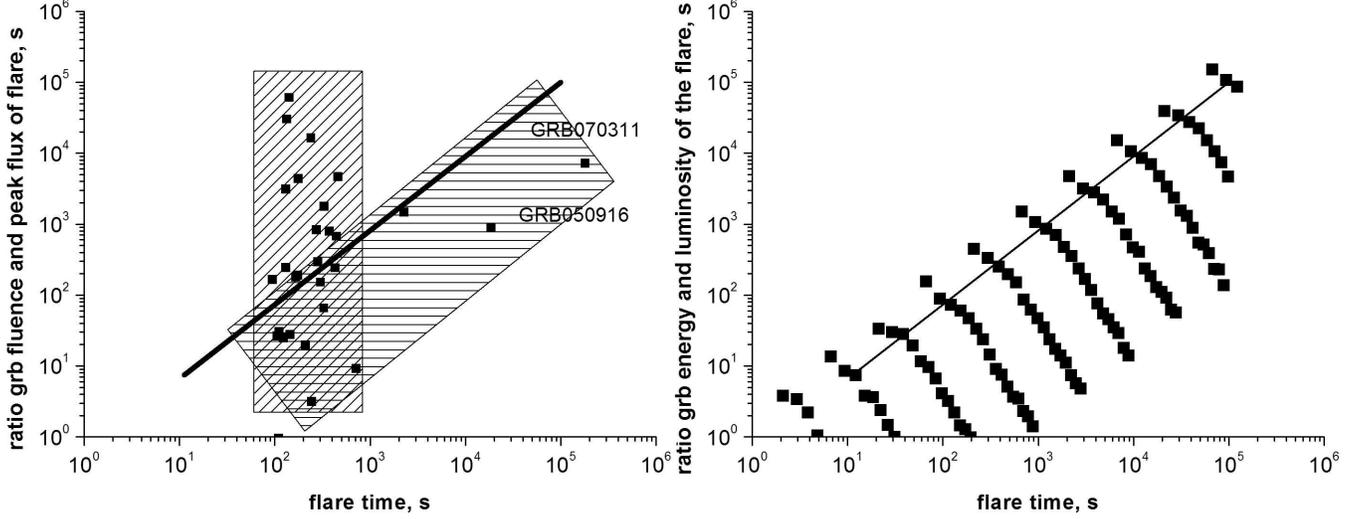The statistic properties of modeling precursors are presented on Fig.8.

Figure 9. The observed GRB fluence-to-peak-luminosity ratio as a function of flare time (Fig. 9a) based on the data of Lazzati (2005) supplemented with two interesting bursts GRB 060124 (Romano, P et al 2006) and GRB 041116 (Golenetskii, et al GCN2835). Theoretical ratio for simulated gamma-ray bursts (Fig.9b) . In our computations we assume that the core mass is equal to $7M_\odot$ the effective Kerr parameter varies from 2 to 7, and magnetic energy lies between 0.01 to 10^{-7}. The solid line is based on bursts, it corresponds rather accurately to equation $\frac{Fluence_{GRB}}{F_{flare}} = t_{flare}$.
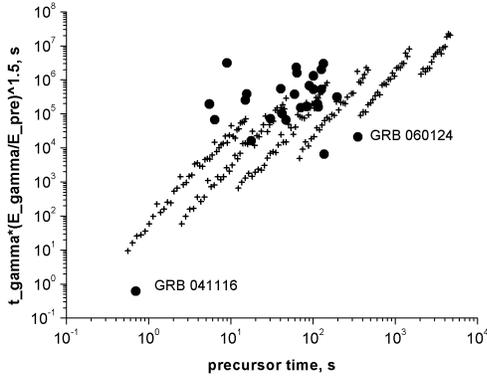
[ht]

Figure 8. The gamma-ray burst time multiplied by the gamma-ray-burst to precursor energy ratio as a function of precursor time. The filled circles show BATSE data (Lazzati, 2002) and the data for two outsending bursts: a short (GRB041116) and a long (GRB 060124) one. We use the fluence data and assume that the opening angles of the precursors are equal to those of the corresponding gamma-ray bursts. The crosses show the simulated gamma-ray bursts with precursors computed for a $7M_\odot$ core. The effective Kerr parameter varied from 7 to 20 , and magnetic field, from $10^{-2} to 10^{-6}$.

We see more or less good similarity between the artificial and observed precursors.

8.2   X-Ray Flares.

If the initial spinar radius R_B is small, the energy release at the time of its formation is sufficient to produce a gamma-ray burst, and hence the first flare should be interpreted as a gamma-ray burst, whereas the secondary release of energy

by the spinar can be interpreted as a flare. In this case the energy of the gamma-ray burst is approximately equal to:

$$E_{GRB} = E_B \approx \frac{GM^2}{2R_B} = \left(\frac{1}{2a_0^2}\right) M_{core}c^2 \tag{50}$$

The burst luminosity is

$$L_{flare} = \frac{\mu_g^2}{R_g^3}\omega_g \tag{51}$$

where μ_g and ω_g are the magnetic moment and angular velocity at the distance of R_g, respectively:

$$\mu_g \sim \mu_0 \frac{Rg}{R_0} \qquad \omega_g \sim \omega_0 \left(\frac{R_0}{Rg}\right)^2$$

Hence the time gap between the gamma-ray burst and the flare is equal to the spin-down time of the spinar at the maximum radius:

$$t_{flare} \sim I_B\omega R_B^3/\mu_B^2$$

Simple substitutions yield the following relation between the observed flare parameters:

$$L_{flare} = \frac{E_{GRB}}{t_{flare}}(\frac{R_B}{Rg})^{5/2} \sim \frac{E_{GRB}}{t_{flare}}\left(\frac{Mc^2}{E_{GRB}}\right)^{5/2} \tag{52}$$

We now substitute the observed quantities into the latter formula to obtain:

$$\frac{Fluence_{GRB}}{F_{flare}} = \left(\frac{\theta_{flare}^2}{\theta_{GRB}^2}\right)\left(\frac{Mc^2}{E_{GRB}}\right)^{-5/2} t_{flare} \tag{53}$$

whereF_{flare} is the maximum flux during the flare and $Fluence_{GRB}$ is the total fluence of the gamma-ray burst.

In the latter relation E_{GRB} is the only quantity that depends on the distance to the gamma-ray burst. We can therefore plot the observed relation $Fluence_{GRB}/F_{flare} = function(t_{flare})$. Figure 9 shows the observed relation and
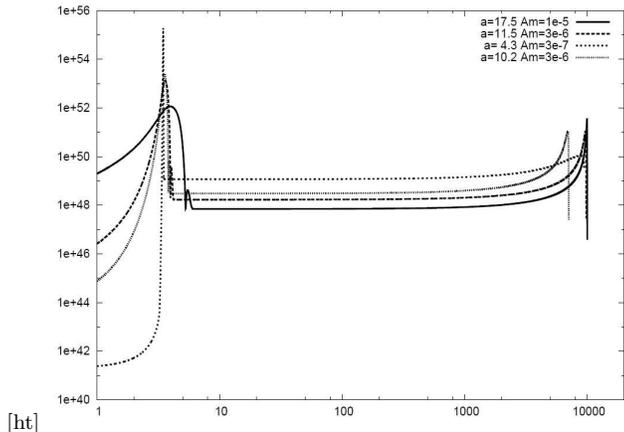
[ht]

Figure 10. Computed energy release during the process of collapse with low angular momentum and weak magnetic field.

[ht]

Figure 11. Experimental Swift X-Ray light curve of the long curve on the x-ray plateau (Troja et al. (2007))and theoretical model luminosity with parameters: $Umag/Ug = 10^{-7}$ and effective Kerr parameter $a = 2.0$ (black line).

the relation simulated in our model. We adopt experimental data from Chincarini et al. (2007). The straight line shows approximate analytical relation (53) :

Figure 9b shows our computed models for the collapse of 7-solar mass star with parameters:

$$2 < a < 20$$
$$10^{-7} < \alpha_m < 10^{-2}$$

One can see that the observed and theoretical spectra show similar trends for the part of the flares (inclined rectangle): they both grow toward (temporally) distant flares with a comparable scatter. The scatter is mostly due to the large factor, and the difference between the mean values is due to the following ratio

$$\left(\frac{\theta_{flare}^2}{\theta_{GRB}^2}\right)\left(\frac{Mc^2}{E_{GRB}}\right)^{-5/2} \sim 10 \tag{54}$$

When converting XRT observations we assumed that *1 count/s=10^{-10}* (Sakamoto et al. 2006, GCN Report 19.1 02Dec06)

One must bear in mind, when comparing the observed and simulated points, that BAT and XRT soft-ray detectors operate in different energy intervals. XRT observations are made in the energy interval $0.3 - 10keV$, where absorption may be important. In addition, the observed fluxes during flares must be multiplied by a factor of five to seven, because the spectrum has a power-law form and is much wider than the XRT energy channel. Moreover, part of the flares (especially those with delays $< 100s$) can also be explained by the emission of a system of shocks (reverse shock Chincarini et al., (2007)).

All this leads us to conclude that the slope and scatter of the average theoretical and observational curves agree well with each other (for part of the flares) and the absolute vertical shift may be due to the differences of the directivity diagrams of the gamma-ray burst and optical flare, soft x-ray extinction, and extrapolation of the power-law spectrum to a wider energy interval.
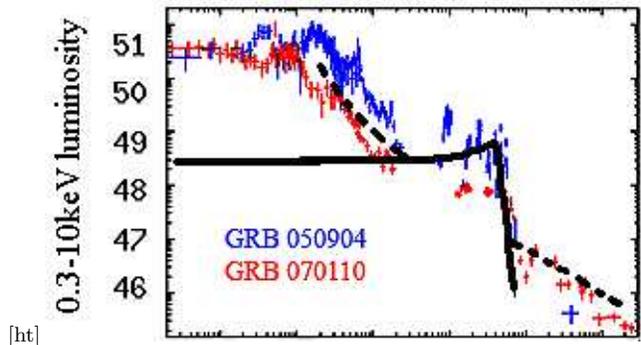
9   AN EXTRAORDINARY LONG X-RAY PLATEAU GRB070110 AND GRB050904.

Two of several hundred gamma-ray bursts — GRB070110 and GRB050904 — do not fit the common scenario of the X-Ray afterglow formation. Both bursts exhibit a long plateau with a rest-frame duration of $6000 - 7000s$. Troja et al. (2007) associated such a long activity with the specifics of the central engine and, in particular, with the formation of a neutron star after the collapse of a low-mass core (with the mass below the Oppenheimer—Volkoff limit).

We fully agree that such an unusual behavior of the X-ray afterglow is due to the central engine, but we believe that the plateau appears not as a result of the radiation of the neutron star, but as a result of the activity of a spinar with anomalously weak magnetic field. An hypothesis Troja, E., et al. (2007) associates the plateau with the collapse producing a neutron star – a radio pulsar – whose activity becomes appreciable during the fading of the afterglow. We believe this interpretation of the plateau to be too far fetched. The intensity of the magnetodipole radiation, which is typical for radio pulsars, decreases with time as t^{-2}. The abrupt termination of the plateau stage remains completely unexplained in the young pulsar model. The authors of this hypothesis point out that the decrease of luminosity could be a result of generation of the magnetic field. However, the last assumption makes the model too complicated.

A plateau with a slight increase and abrupt decrease of luminosity appears naturally in the spinar paradigm.

In our scenario a plateau is a flare with weak magnetic field. In other words, in this case the gamma-ray burst corresponds to the halt of the collapse by centrifugal forces at radius R_B, and the plateau is an extended flare due to magneto-rotational losses.

Let us first make some approximate estimates. The initial Kerr parameter is equal to:

$$A_0 = \frac{I\,\omega\,c}{GM^2} \tag{55}$$

The initial spinar radius is:

$$R_s = \frac{a^2 GM}{c^2} = \frac{1}{2}a^2\,Rg \tag{56}$$
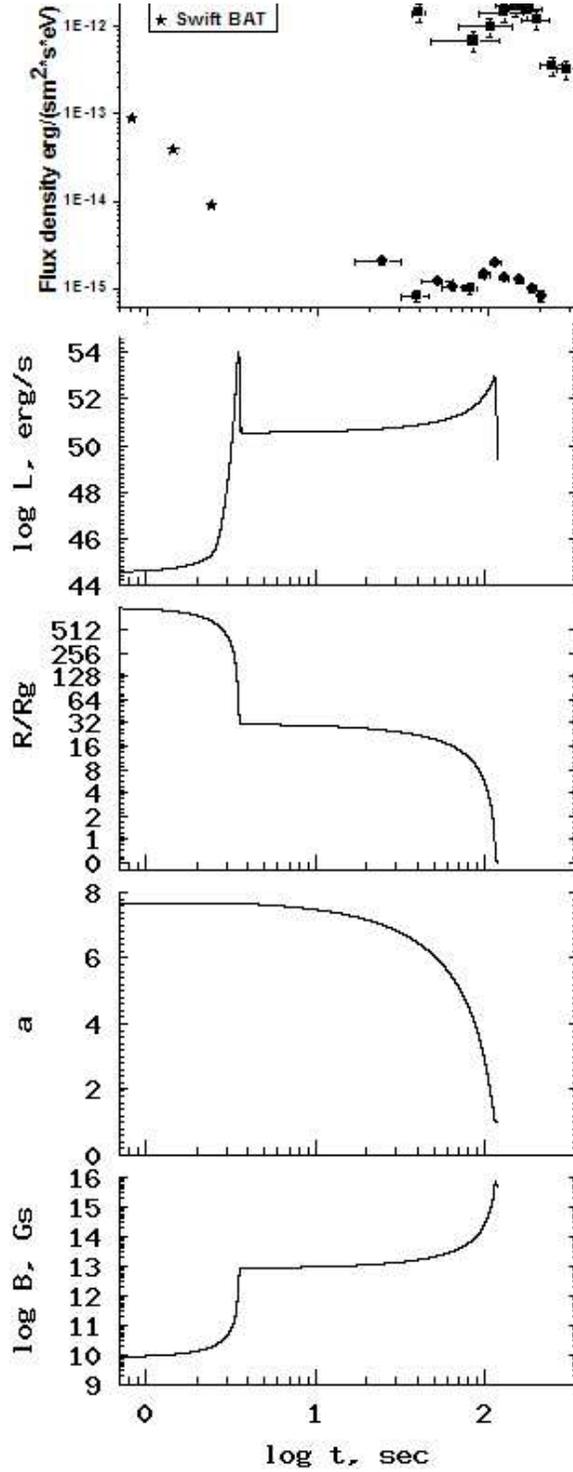
The energy of the gamma-ray burst is

Figure 12. Light curve and theoretically computed luminosity,radius , effective Kerr parameter, and magnetic field for GRB060926. The initial parameter for theoretical computation is $a_0 = 7.6$ and $\alpha_m = 10^{-4}$.

$$E_{GRB} = \frac{1}{2}\frac{GM^2}{R_s} = \frac{Mc^2}{2a^2} \qquad (57)$$

We derive from this relation the Kerr parameter:

$$a = E_{GRB}/Mc^2 \qquad (58)$$

The characteristic plateau duration is determined by the time scale of the loss of the spinar angular momentum:

$$t_{plato} = t_{flare} = \frac{I_B \omega_B}{\kappa_t \frac{\mu^2}{R_B^3}} \sim \frac{GMa^3}{2\kappa_t c^3 \alpha_m} \qquad (59)$$

The luminosity of the plateau at its maximum computed without the allowance for relativistic effects is:

$$L_{plato}(\text{max}) \sim \frac{\alpha_m \kappa_t}{4x}\frac{c^5}{G} \qquad (60)$$
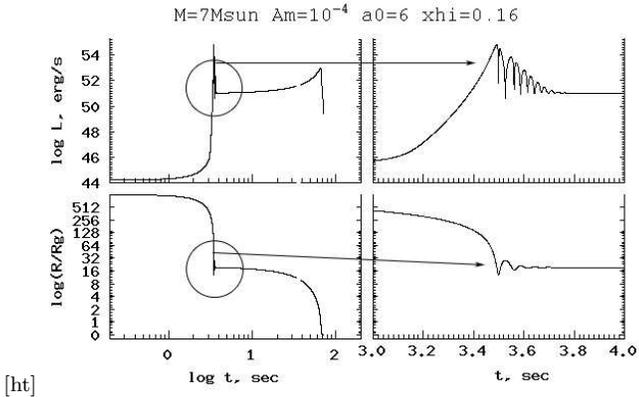
M=7Msun Am=10⁻⁴ a0=6 xhi=0.16

Figure 13. Computed collapse of a $7M_\odot$ core. Qualitative illustration of the fine structure of the temporal behavior of the gamma-ray burst or multiple precursors.

We now use the observed plateau time to derive the parameters of the collapse:

$$\alpha_m = \frac{GMa^3}{2\kappa_t c^3 t_{plato}} \sim 10^{-8} \left(\frac{M}{10M_\odot}\right) t_4^{-1} a^3 \kappa_t^{1/3} \qquad (61)$$

Figure 10 shows the theoretical curve of the luminosity spinar evolution for different initial parameter. This spinar light curve shows a characteristic plateau whose luminosity and duration are totally consistent with experimental data (Troja et al., 2007). So the plateau appears naturally in the spinar model and it is a typical feature for the collapse of a core with small angular momentum and weak magnetic field, and may be find in many different cases.

To illustrate these points, we computed a best theoretical light curve ($\alpha_m = 10^{-7}, a = 2.0$) artificially supplying additional self-similar radiation in accordance with the following law (Fig.11) and preview if with experimental data given by Troja et al. (2007):

$$F = F_{theory} + C_1 t^{-2} + C_2 t^{-1}$$

10   GRB 060926

X-ray flares can sometimes also be observed at optical wavelengths. Let us try to explain the phenomenon of such a flare in the gamma-ray burst GRB 060926, where an optical flare was discovered along with the x-ray flare. We choose this burst not only because we want to illustrate how spinar paradigm works for flares observed both at x-ray and optical wavelengths, but also because the optical radiation of this burst was discovered by MASTER group whose members include the authors of this paper.

Optical observations of the gamma-ray burst GRB060926 recorded by Swift gamma-ray observatory (Holland,S et al 2006) were performed with MASTER telescope operating in an automatic mode under good weather conditions (Lipunov et al 2006). The first exposure started at 16:49:57 UT 2006-09-26, $76s$ after the gamma-ray burst was recorded. We found in the first and subsequent coadded frames an optical transient with the following coordinates:

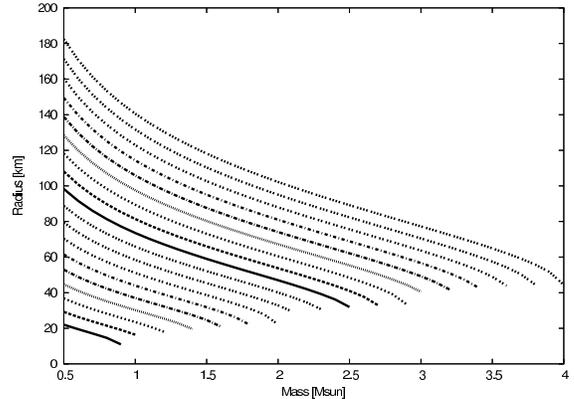$$\alpha = 17^h 35^m 43^s.66$$
$$\delta = 13^d 02^m 18^s.3$$

Figure 14. Show the radius of a nonrotating neutron star depends on its mass for various values of parameter b that appears in our equation of state.

$$err = \pm 0^s.7''$$

which agree with the coordinates of the optical transient discovered by Holland et al. (2006) within the errors of our observations. The results of the corresponding photometry yielded the first data points on the light curve.

We found an optical flare event — after a short decrease the brightness began to rise beginning with the 300th second and reached its maximum near $500--700s$. Synchronous X-ray flux measurements with Swift XRT show a similar event (see Fig.12). Note that the absorption determined from x-ray data corresponds to a column density of $n_H = 2.2 10^{21} cm^{-2}$ of which $n_H = 7 10^{20} cm^{-2}$ is Galactic absorption (Holland et al. 2006). Given the redshift $z = 3.208$, the total absorption in our band is equal to three magnitudes. We naturally assume that the dust-to-hydrogen ratio is the same as in our Galaxy. A comparison of our optical measurements with the x-ray fluxes measured by Swift XRT (Holland et al. 2006) allowed us to determine the slope of the spectrum, which we found to be constant within the errors and equal to $\beta = 1.0 \pm 0.2$:

$$F \sim E^{-\beta} [erg/cm^2 s\, eV] \qquad (62)$$

The spectrum obtained agrees with the x-ray spectrum within the errors (Holland,S et al 2006).

Such a phenomenon was already observed at least in several cases: GRB060218A z=0.03 (Quimby et al, 2006a, GCN4782) at the 1000th second, GRB060729 z=0.54 at the 450th second (Quimby et al., 2006b,c GCN 5366,5377), GRB060526 z=3.21 at the 188th second (Dai X. et al 2007), and also during the bursts GRB990123, GRB041219a, GRB060111b (Wei D.M., 2007) , etc.

Note that the gamma-ray burst that we discuss here has a redshift of 3.208 (V.D'Elia et al GCN5637). Figure 12b-e shows the results of optical and X-ray observations of the flare and of the theoretical computations of a spinar with parameters $a_0 = 7.6$ and $\alpha_m = 10^{-4}$.

Note also that redshift dilates all time intervals by a factor of $(1+z)$ and therefore we show all experimental light curves reduced to the rest-frame. We hence have to explain a flare at the $\sim 100^{th}$ second, which is about 50 times weaker than the gamma-ray burst as we illustrate in Fig.12.
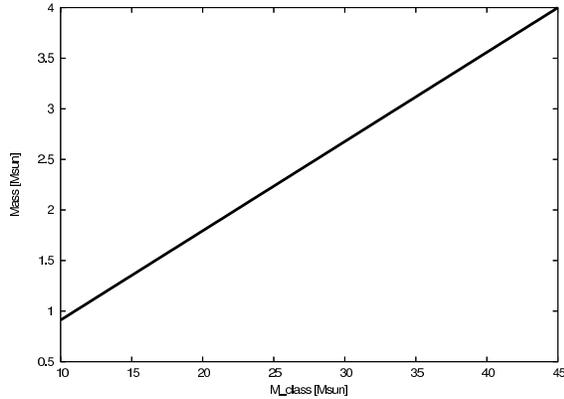
[ht]

Figure 15. The Oppenheimer—Volkoff limit as a function of parameter M_{Class} $see(eq.29)$ that appears in our equation of state (28) for a nonrotating neutron star.

11   DISCUSSION

Our proposed non-stationary model developed in terms of the Spinar Pardigm of magneto-rotational collapse is physically transparent. It takes into account all the main relativistic effects and allows their impact on the operation of the central engine and on the accompanying events to be estimated. It goes without saying that this model cannot replace precise magnetohydrodynamic computations, but it evidently helps to choose the inevitable simplifications for such computations.

The central assumption in our model is that dissipation of the angular momentum of the collapsing core is due to magnetic field. It is clear that turbulent viscosity and generation of Alfven waves may play important part in the real situation. However, on the one hand, no simple physical model has so far been developed for these events and, on the other hand, the magnetic field that we introduce can be viewed as some effective parameter describing viscous loss of momentum. We point out that although we use dipole moment in our set of equations of motion, they actually do not assume the dipole nature of the magnetic field. This remarkable circumstance is due to the fact that the spin-down torque μ^2/R_c^3 that we use here coincides with the energy of magnetic field, $U_m \approx \mu^2/R_c^3$, for a spinar whose radius is equal to the corotation radius $R = R_c$. By the way, this fact proves that we adopted maximally effective spin-down magnetic moment.

To reduce the number of initial hypotheses, we never allowed for the possible generation of magnetic field (Kluznuzk & Ruderman, 1998) as a result of differential rotation of the collapsing core. On the other hand, generation of magnetic field can be easily incorporated into the approximation employed. It can be done should theory clearly disagree with observations.

There are other phenomena capable of complicating the picture described above. For example, the spinar may at a certain time break into two objects during the collapse of a rotating core (Berezinski et al.,1988; Imshennik, 1992). We do not yet consider the second possibility, which, in principle, may result in the appearance of several flares or precursors around the gamma-ray burst.
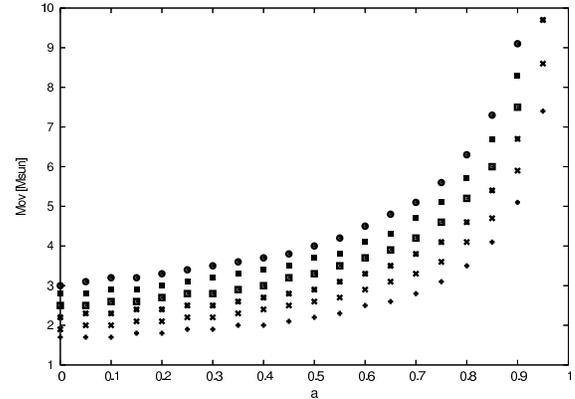
[ht]

Figure 16. The Oppenheimer—Volkoff limit as a function of the velocity of rotation of the neutron star (in the units of the Kerr parameter).

The problem of precursors and flares requires a separate explanation. On the one hand, we stress that close precursors and flares may result from the presence of a complex system of shocks in the relativistic jet. On the other hand, the phenomenon of multiple precursors can be easily explained by the oscillations of the newborn spinar at the centrifugal barrier. We artificially suppressed these oscillations by introducing a special dissipative force with the dissipation time scale parameter. As we showed above, we can obtain up to 10 precursors for a single gamma-ray burst if we choose the dissipation time scale to be one order of magnitude longer than the period of spinar rotation (Fig.13).

However, the description of fine effects lies beyond the scope of this paper.

We assume that interpreting shock events accompanying the gamma-ray bursts in terms of a simple two-parameter scheme is an important step toward understanding the operation of the central engines of the gamma-ray bursts.

Appendix 1. Parameters of neutron stars with equation of state (28).

To choose the most appropriate constants in approximate equation of state (28), we analyze the global properties of neutron stars in accordance with dynamic equation (24), which in the static case transforms into the following simple equation:

$$\frac{4}{Rg^2}\frac{GM}{x^3}\frac{(x^2-2ax+a^2)^2}{(\sqrt{x}(x-2)+a)^2} - \omega^2 R - \frac{P}{R} = 0 \qquad =>$$

$$\frac{R}{2MGRg}\frac{(4M^2G^2-2MG\omega c\sqrt{2Rg^2R}+Rg^2R^2\omega^2c^2)^2}{(2MG\sqrt{2\frac{R}{Rg}}(R-Rg)+RgR^2\omega c)^2} - \omega^2 R - \frac{P}{R} = 0$$

Figure 14 shows the dependence of the radius of a non-rotating neutron star on its mass for various values of parameter b, which appears in our equation of state. First, we see natural decrease of the star's radius with increas-

ing mass, which is typical of self-gravitating configurations with equilibrium maintained by the pressure of ideal degenerate gas. However, this is of minor importance for us compared to the fact that the radii of neutron stars of reasonable $(1.5 - 3M_\odot)$ masses lie within reasonable limits: from 20 to 100 km. Figure 15 shows the dependence of the Oppenheimer—Volkoff limit on our parameter b. The available orthodox model equations of state for neutron stars predict that the maximum mass of a neutron star is $1.5 - 3M_\odot$. This corresponds to the following interval of parameter b: Fig. 16 demonstrated Oppenheimer—Volkoff –limit depend on effective Kerr parameter.

$20M_\odot < b < 35M_\odot$

Fig. 16 demonstrated Oppenheimer—Volkoff —limit depend on effective Kerr parameter.

REFERENCES

Artemova, I.V., Bjornsson and Novikov, I.D., 1996, Ap.J., 461, 565-571

Berezinskii,V.S., Castagnoli,C.,Dokuchaev,V.I.,Galeotti,P,1988, Nuovo Cimento C, Serie 1, 11 C, 287

Bisnovatyi-Kogan, G.S., 1971 SvA. 14, 652

Bisnovatyi-Kogan, G.S. & Blinnikov, S.I., 1972, Ap&SS, 19, 119

Chincarini, G., Moretti, A., Romano, P. et al., 2007, astro-ph/0702371vl

Dai X. et al., 2007, ApJ, 658, 509

D'Elia V. et al. 2006,: GCN 5637

Duez, M.D., Liu, Y.T., Shapiro, S.L. and Stephens, B.C., 2005, Phys.Rev. D 72, 024028

Duez, M.D.; Liu,Y.T; Shapiro,S.L.; Shibata,M; Stephens,B., 2006, Phys.Rev. D 73,104015

Friedmon J.L., Ipser J., Parker L., 1985, ApJ, 292,111

Gehrels, N., Norris, J.P., Barthelmy, S.D. et al., 2006, Nat, 444, 1044

Ginzburg, V.L. & Ozernoy, L.M., 1964, JEPT, 47, 1030

Golenetskii S., R.Aptekar, E. Mazets, V. Pal'shin, D. Frederiks, 2006 GCN 2835

Granot, J., Revista, 2007 Mexicana de Astronomía y Astrofísica (Serie de Conferencias) Vol. 27, pp. 140-165

Holland, S. T. & Barthelmy, S. D. et al., 2006 GCN 5612

Holland, S.T., Barthelmy, S.D., Barbier, L.M. et al., 2006 GCN Report, 1.1 02oct06

Hoyle, F. & Fowler, W.A., 1963, MNRAS, 125, 169

Imshennik, V.S., 1992, Pis'ma Astron. Zu.; 18, 489

Kluznuzk, W. & Ruderman, M., 1998, ApJ., 505, L113

Lazzati,D.2005, MNRAS, 357, 722

LeBlanc, J.H. & Wilson, J.R., 1970, ApJ, 161, 541

Lipunov, V.M.,1983, Ap&SS., 97, 121

Lipunov, V.M.,1987, Ap&SS., 132, 1

Lipunov, V.M., 1992, "Astrophysics of Neutron Stars", Springer-Verlag, Berlin.

Lipunov, V.M. & Panchenko, E.I., 1996, A&A., 312, 937-940

Lipunov, V.M. & Gorbovskoy E.S, 2007., ApJL, 665, L97 (astro-ph/0705.1648v2)

Lipunov,V.; Kornilov,V.; Kuvshinov,D.; Tyurina,N.; Belinski,A.; Gorbovskoy,E.; Krylov,A.; Borisov,G.; Sankovich,A.; Vladimirov,V.; Gritsyk,P. 2006. GCN. 5632.

Lipunova, G.V.,1997, Astronomy Letters, Volume 23, pp.84-92

Lipunova, G.V. & Lipunov, V.M., 1998, Astron.Astrophys., v.329, p.L29-L32

Manko, V.S. and Sibgatullin, N.R., 1992, Class.Quantum Grav., Vol.9, L87-L92

Moiseenko,S.G.; Bisnovatyi-Kogan,G.S.; Ardeljan,N.V, 2006 MNRAS. 370, 31, 501

Morrison P., 1969 ApJL 157, 73

Mukhopadhyay, B., 2002, ApJ, 581,427

Narayan, R., Piran, N.,Kumar, P., 2001, ApJ, 557,949

Novikov, I.D., 1964, AZh., 41, 290 (in Russian)

Ostriker, J.P. 1970, Acta Phys. Acad. Sci, 29, 69

Ozernoy, L.M., 1966, SvA, 10, 241

Ozernoy, L.M. & Usov, V.V., 1973, Ap&SS., 25, 149

Quimby R., B. E. Schaefer, H. Swan, 2006 gcn 4782

Quimby R., H. Swan, W. Rujopakarn, D.A. Smith, 2006 GCN 5366

Quimby R. & E. S. Rykoff, 2006 GCN 5377

Ramirez-Ruiz, E., Celotti, A. & Rees, M. 2002, MNRAS, 337, 1349

Romano, P.; Campana, S.; Chincarini, G. et al 2006 *A&A, 456 917*

Thorne, K.S., Price, R.H. and Macdonald, D.A. , 1986, Black Holes: The Membrane Paradigm, Yale University Press, New Haven and London

Paczynski, B.,1986, ApJ, 308, L43

Paczynski, B. & Wiita, P.J., 1980, A&A, 88, 23.

Piran, , T. 2005, Rev. Mod. Phys., 76, 1143

Sakamoto et al. 2006, GCN Report 19.1 02Dec06

Troja, E., Cusumano, G., O'Brien, P., 2007, et al. , ApJ(in press), (astro-ph/0702220vl)

Vietri, M. & Stella, L., 1998, ApJ, 507, L4

Woosley, S., 1993, ApJ, 405, 273

Woosley, S. & Zang, B., 2007, Proc. of Roy.Soc. meeting on GRB, astroph/0701320

Wang, Xiang-Yu & Meszaros, P., 2007, astro-ph/0702441v1

Waxman, E. & Meszaros, P., 2003, ApJ, 584, 390

Wei D.M., 2007, MNRAS, Volume 374, Issue 2, 525

Zel'dovich, Ya., B., Blinnikov, S.I., Shakura, N.I. 1980 "The theory of a structure and evolution of stars", Moscow State University Press, Moscow, p.160 (in Russian)